Thermal and Light-Induced Spin Transition in the High- and Low-Temperature Structure of $[Fe_{0.35}Ni_{0.65}(mtz)_6](ClO_4)_2$

Th. Buchen,*,† D. Schollmeyer,‡ and P. Gütlich

Institut für Anorganische Chemie und Analytische Chemie, Johannes Gutenberg Universität Mainz, Staudingerweg 9, D-55099 Mainz, Germany

Received April 13, 1995[⊗]

The thermal and light induced spin transition in $[Fe_{0.35}Ni_{0.65}(mtz)_6](ClO_4)_2$ (mtz = 1-methyl-1*H*-tetrazole) was studied by ^{57}Fe Mössbauer spectroscopy and magnetic susceptibility measurements. In addition to the spin transition of the iron(II) complexes the compound undergoes a structural phase transition. The high-temperature structure could be determined by X-ray crystallography of the isomorphous $[Fe_{0.25}Ni_{0.75}(mtz)_6](ClO_4)_2$ complex at room temperature. The X-ray structural analysis shows this complex to be rhombohedric, space group $R\bar{3}$, with a = 10.865(2) Å and c = 23.65(1) Å with three molecules in the unit cell. The transition to the low-temperature structure occurs at ∼60 K without changing the spin state of the molecules. By subsequent heating of the complex the high-temperature structure is reached again between ca. 170 and 200 K. The spin transition behavior is strongly influenced by the structural changes, and the observed spin transition curves are completely different for the high- and low-temperature phases. In the high-temperature structure a complete and gradual spin transition between 220 and 120 K ($T_{1/2}(\gamma_{HS} = 0.5)$ = 185 K) is detected; the high-spin (HS) state is represented by one HS doublet in the Mössbauer spectra. In the low-temperature structure a two-step transition curve is detected in the heating mode. About 36% of the molecules show a LS (low-spin) → HS transition between ca 50 and 75 K. Then the HS fraction stays constant up to 150 K. A further increase in the high-spin fraction is observed at temperatures above 150 K. In this structural phase the HS state is represented by two different HS doublets in the Mössbauer spectra. The formation of metastable HS states by making use of the LIESST effect is only possible in the low-temperature structure. By excitation of the LS molecules with green light, two different HS states are populated which show very different relaxation behavior. One HS state shows a relaxation to the LS state even at 10 K; the other HS state shows a very slow HS → LS relaxation at 60 K (within days), leading to the HS fraction corresponding to the thermal equilibrium value.

1. Introduction

Thermal and light-induced spin transition is a well-established phenomenon in the coordination chemistry of iron(II).[1−4] The phenomenon occurs in solution as well as in the solid state. In solution gradual transitions are observed which can be understood in terms of a Boltzmann distribution over the vibronic levels of the high-spin (HS) and the low-spin (LS) state. In the solid state, however, a great variety of spin transition curves, given as the HS fraction γ_{HS} as a function of temperature, are detected. Gradual as well as steep transitions with and without hysteresis are observed. The different types of spin transition curves are a consequence of the cooperative nature of the spin transition phenomenon in the solid state. The origin of the interaction mechanism between the spin-changing molecules is still under debate. The model of Spiering et al.,[5−7] which is based on the observation that the volumes of the HS and LS complexes are quite different due to the decrease of the iron−ligand bond lengths in the course of the spin transition, was successfully applied to the spin transition behavior in a number of complexes of the general formula $[Fe(pic)_3]X_2$·Sol (pic = 2-picolylamine; X = Cl^-, Br^-; Sol = EtOH, MeOH)[8,9] where the spin transition is not associated with further structural changes of the compounds. In many compounds, however, the spin transition is accompanied by additional structural changes. For these compounds large hysteresis effects in the γ_{HS} vs T curve are reported, and in some of these complexes it was possible to generate metastable HS states by rapid cooling of the sample due to the slow kinetics of the additional phase transition.[10−12] The relaxation of the metastable HS state which is observed by subsequent heating of the compound to a certain temperature region is then governed by the kinetics of the phase transition.[12] In these compounds where, in addition to the normal shortening of the iron(II)−ligand bond lengths in the course of the spin transition, the spin crossover is accompanied by further structural changes one has to differentiate between electronic and crystal structural changes, but obviously both effects can influence each other.

In the course of our studies on metal-diluted iron tetrazole complexes we found that the spin transition in $[Fe_{0.35}Ni_{0.65}(mtz)_6](ClO_4)_2$ is strongly influenced by an additional structural phase

† Present address: Department of Chemistry, Odense University, Dk-5230 Odense, Denmark.

‡ Present address: Institut für Organische Chemie, Johannes Gutenberg Universität Mainz, D-55099 Mainz, Germany.

⊗ Abstract published in *Advance ACS Abstracts,* November 15, 1995.

(1) Gütlich, P.; Hauser, A.; Spiering, H. *Angew. Chem., Int. Ed. Engl.* **1994**, *33*, 2024.
(2) Toftlund, H. *Coord. Chem. Rev.* **1989**, *94*, 67.
(3) König, E. *Struct. Bonding* **1991**, *76*, 53.
(4) Hauser, A. *Coord. Chem. Rev.* **1991**, *111*, 275.
(5) Spiering, H.; Meissner, E.; Köppen, H.; Müller, E. W.; Gütlich, P. *Chem. Phys.* **1982**, *68*, 65.
(6) Willenbacher, N.; Spiering, H. *J. Phys. C: Solid State Phys.* **1988**, *21*, 1423.
(7) Spiering, H.; Willenbacher, N. *J. Phys. Condens. Matter* **1989**, *1*, 10089.
(8) Adler, P.; Wiehl, L.; Meissner, E.; Köhler, C. P.; Spiering, H.; Gütlich, P. *J. Phys. Chem. Solids* **1987**, *48*, 517.
(9) Jakobi, R.; Spiering, H.; Wiehl, L.; Gmelin, E.; Gütlich, P. *Inorg. Chem.* **1988**, *27*, 1823.
(10) Ritter, G.; Kïnig, E.; Irler, W.; Goodwin, H. A. *Inorg. Chem.* **1978**, *17*, 224.
(11) Goodwin, H. A.; Sugiyarto, K. H. *Chem. Phys. Lett.* **1987**, *139*, 470.
(12) Buchen, Th.; Gütlich, P.; Goodwin, H. A. *Inorg. Chem.* **1994**, *33*, 4573.

0020-1669/96/1335-0155$12.00/0

change. But in contradiction to other examples where the additional structural changes lead only to a broad hysteresis in the spin transition curve, the observed spin transition behavior in the high- and low-temperature phases of the complex under study is completely different.

In this paper we report on the spin transition behavior in both high- and low-temperature structural phases. The high-temperature structure of the complex was determined by X-ray crystallography of the isomorphous $[Fe_{0.25}Ni_{0.75}(mtz)_6](ClO_4)_2$ complex. LIESST (light-induced excited spin state trapping) experiments were performed in the low-temperature structure.

2. Experimental Section

Caution! Although no problems were encountered in the preparations of the following complexes as perchlorate salts, suitable care should be taken when handling such potentially hazardous compounds.

2.1. Sample Preparation. 1-methyl-1*H*-tetrazole (mtz) was prepared as described earlier.[13] $[Fe(mtz)_6](ClO_4)_2$ and $[Ni(mtz)_6](ClO_4)_2$ were obtained from equimolar concentrated aqueous solutions of $[Fe(H_2O)_6](ClO_4)_2$ and $[Ni(H_2O)_6](ClO_4)_2$, respectively, and the ligand under nitrogen. The volume of this solution was carefully reduced at room temperature until the complex crystallized out. The raw product was filtered and dried. It was further purified by dissolving the material in dry nitromethane and evaporating the solvent with an oxygen-free and dry nitrogen stream. Mixed crystals of $[Fe_xNi_{1-x}(mtz)_6](ClO_4)_2$ were obtained by dissolving $[Fe(mtz)_6](ClO_4)_2$ and $[Ni(mtz)_6](ClO_4)_2$ in nitromethane and evaporating the solvent, as described above. Due to the different solubility of the complexes, small fractions of the precipitated crystals were separated to avoid inhomogeneous distributions of the iron and nickel complexes within one fraction. In this way 12 fractions of $[Fe_xNi_{1-x}(mtz)_6](ClO_4)_2$ mixed crystals with an iron content ranging from $x = 0.25$ for the first fraction to $x = 0.934$ for the last fraction were obtained. The relative iron content of the samples was determined by X-ray fluorescence analysis using a Philips PW1400 X-ray fluorescence spectrometer. The purity of the complexes was controlled by routine elemental analysis.

2.2. Susceptibility Measurements. The magnetic susceptibility $\chi(T)$ of the mixed crystals of $[Fe_xNi_{1-x}(mtz)_6](ClO_4)_2$ between 20 and 295 K was measured with a Foner type magnetometer, equipped with a helium flow cryostat, in an external field of 1 T. The paramagnetic correction for the nickel complex was determined by measuring $\chi(T)$ of the $[Ni(mtz)_6](ClO_4)_2$ complex. The diamagnetic corrections for the ligands were obtained from Pascal constants. The HS fraction as a function of temperature was calculated from the measured susceptibilities assuming Curie−Weiss behavior for the pure compound in the HS state and temperature independent paramagnetism for the LS state.

2.3. Mössbauer Spectroscopy. Mössbauer spectra of $[Fe_{0.35}Ni_{0.65}(mtz)_6](ClO_4)_2$ were recorded between 5 and 295 K with a conventional Mössbauer spectrometer. The $^{57}Co/Rh$ source was kept at room temperature. All isomer shifts in this work refer to the source. The samples were sealed in polished plexiglass containers (3 cm^2, ca. 7 mg Fe cm^{-2}) and mounted in a helium flow cryostat (CF 506, Oxford Instruments). The cryostat was equipped with windows of transparent Mylar foils. The samples were irradiated with a Xe-arc lamp using a water bath as IR filter. For LIESST experiments a filter with maximum transmission between 350 and 650 nm was used, and for reverse LIESST experiments a filter translucent for $\lambda \geq 700$ nm was used. A carbon/glass resistance was directly mounted at the sample holder to control the temperature during irradiation. The Mössbauer spectra were fitted to Lorentzians using the program MOSFUN[14] assuming equal Debye−Waller factors for the HS and LS states.

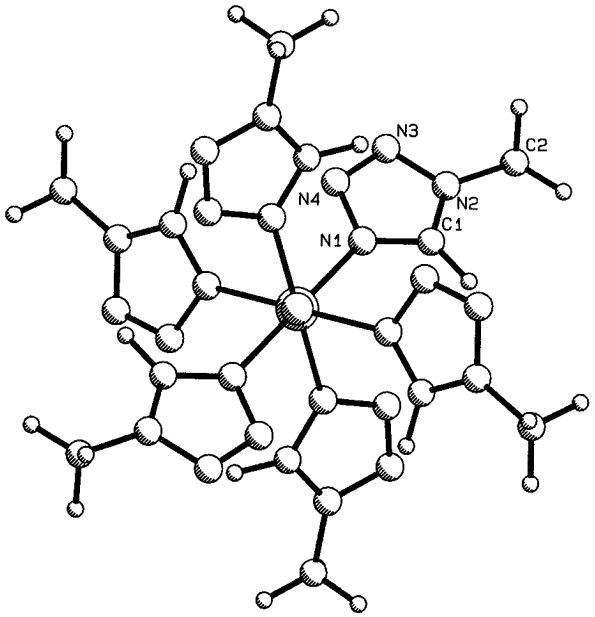

Figure 1. Configuration of the $[Fe_{0.25}Ni_{0.75}(mtz)_6]^{2+}$ cation and numbering scheme of atoms.

2.4. Crystal Structure. 2.4.1. X-ray Measurement. The space group was obtained from rotation and Weissenberg photographs. Intensity data were collected by employing a four-circle diffractometer (CAD4/Enraf-Nonius) at room temperature. Measurements were performed with Mo Kα radiation (graphite monochromator), $\omega/2\theta$ scan up to an angle of $\theta = 30°$ ($0 < h < 13$, $0 < k < 13$, $-33 < l < 33$) with Friedel pairs, maximum scan time 90 s/reflection. The intensities were Lp-corrected.

2.4.2. Solution and Refinement. The positions of all non-hydrogen atoms were determined from a Patterson synthesis (SHELX86).[15] The hydrogen atoms of the tetrazole rings could be determined by difference Fourier syntheses. The hydrogen positions of the methyl group had to be calculated. The structure was refined using SHELX76.[16] Scattering factors were used for C, N, O, and H from SHELX76 and for Ni, Fe, and Cl from Doyle and Turner;[17] anomalous scattering factors were taken from Cromer and Liberman.[18] All non-hydrogen atoms were calculated anisotropically; the hydrogen atoms were calculated isotropically with fixed thermal parameters assuming riding motion. The structure could be refined to an *R* value of 0.054.

3. Results

3.1. Crystal Structure. The moleculare structure of $[Fe_{0.25}Ni_{0.75}(mtz)_6](ClO_4)_2$ shows no significant deviations from standard bond lengths and angles for the ligand, which is almost planar. The octahedral environment of the iron (nickel) ion is slightly distorted (cf. Tables 1−3). The molecular structure of the complex cation with the numbering scheme of the atoms is shown in Figure 1. A projection of the unit cell along the (001) axis is given in Figure 2.

(13) Kamija, T.; Saito, Y. Ger. Offen. P2417023.5, 1971.

(14) Müller, E. W. Ph.D. Thesis, Universität Mainz, 1982.
(15) Sheldrick, G. M. *SHELX86*, Program for the solution of crystal structures; Universität Göttingen, 1986.
(16) Sheldrick, G. M. *SHELX76*, Program for crystal structure determination; University of Cambridge, 1976.
(17) Doyle, P. A.; Turner, P. S. *Acta Crystallogr. Sect. A* **1986**, *24*, 390.
(18) Cromer, D. T.; Liberman, D. J. *J. Chem. Phys.* **1970**, *53*, 1891.

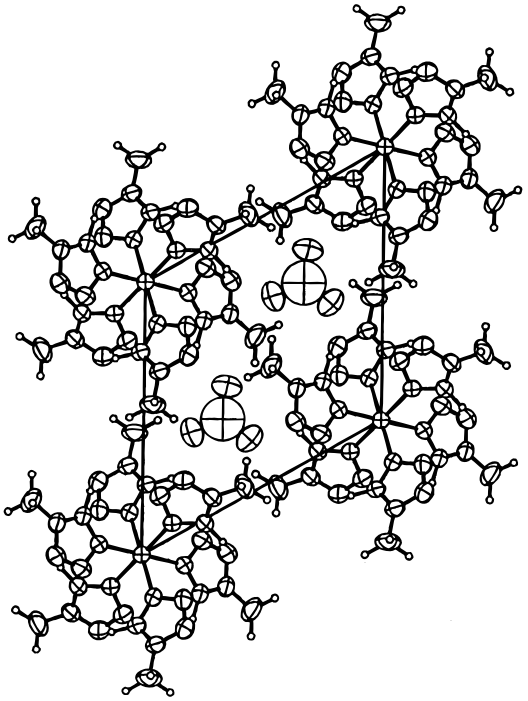

Figure 2. Projection of the unit cell of $[Fe_{0.25}Ni_{0.75}(mtz)_6](ClO_4)_2$ along the (001) axis (thermal ellipsoids with 50% probability).

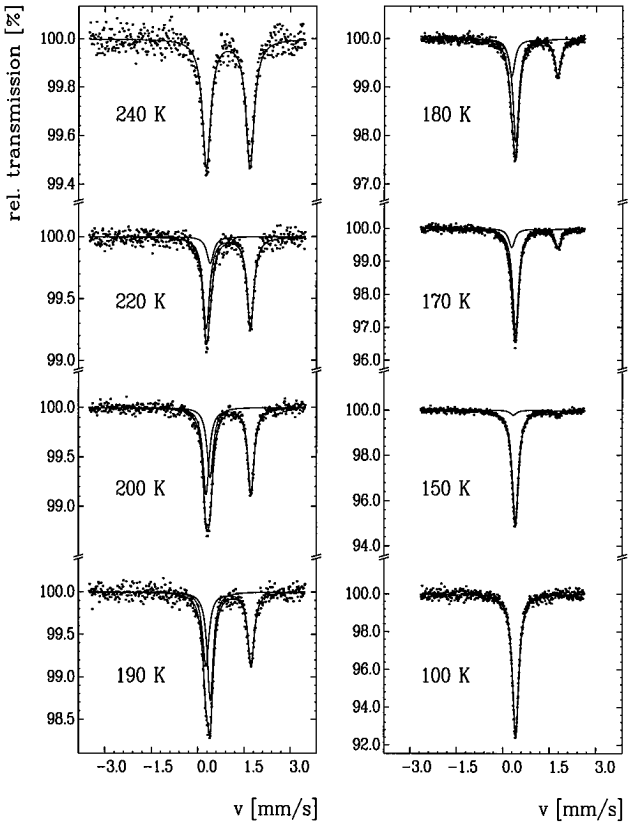

Figure 3. Mössbauer spectra of $[Fe_{0.35}Ni_{0.65}(mtz)_6](ClO_4)_2$ recorded at decreasing temperatures. At 240 K only the resonances of the HS state are observed in the Mössbauer spectrum. With decreasing temperature the resonance line (singlet) of the LS state appears with increasing intensity. At 100 K only the resonance line of the LS state is observed. Thus, the Mössbauer spectra prove a complete spin transition in the cooling direction.

3.2. Thermal Spin Transition. Mössbauer spectra of $[Fe_{0.35}Ni_{0.65}(mtz)_6](ClO_4)_2$ recorded at decreasing temperatures are shown in Figure 3. The Mössbauer spectrum at 240 K shows only one doublet, with an isomer shift of 0.98(1) mm/s and a quadrupole splitting ΔE_Q of 1.41(2) mm/s (cf. Table 4). These Mössbauer parameters are typical of iron(II) in the HS state. With decreasing temperatures an additional resonance line with $\delta \sim 0.41$ mm/s at 220 K (typical for iron(II) in the LS state) is observed. This resonance signal becomes more intense with decreasing temperature, documenting a HS → LS transition of the compound. At 100 K only the LS state is detected in the spectrum. Thus, the Mössbauer spectra clearly prove a gradual and complete spin transition between 240 and 100 K. The results of the Mössbauer investigations were supported by magnetic susceptibility measurements. After correcting for the diamagnetic and paramagnetic contributions from the ligands and the nickel complex, respectively, the derived high-spin fraction $\gamma_{HS}(T)$ yields a spin state conversion curve which is shown in Figure 4. The spin transition is almost complete between 220 and 140 K. It is important to mention that the Mössbauer and magnetic susceptibility measurements have been shown to yield the same spin transition curves in both the heating and cooling mode only if the temperature region is restricted to temperatures higher than ca. 60 K.

If the compound is cooled to 20 K, a very strange behavior is observed. By subsequent heating of the complex, the Mössbauer spectra depicted in Figure 5 were recorded. The iron(II) complexes are still in the LS state at 40 K, but in the temperature range from ca. 50 to ca. 75 K a HS state with an isomer shift of $\delta \sim 1.06$ mm/s and a quadrupole splitting ΔE_Q of ~2.5 mm/s (cf. Table 4) is populated, leading to a HS fraction of ~37% at 80 K. Then the HS/LS ratio remains constant at temperatures up to 150 K, thus leading to a plateau in the spin transition curve. At 150 K an additional HS state is detected with Mössbauer parameters quite similar to the HS state which was observed by initial cooling of the compound (cf. Table 4). To distinguish the two HS states, we shall refer to the HS state with the low and high ΔE_Q values as HS(A) and HS(B), respectively. The intensity of the HS(A) doublet increases with

Table 1. Crystallographic Data for $[Fe_{0.25}Ni_{0.75}(mtz)_6](ClO_4)_2$

chem formula: $C_{12}H_{24}N_{24}Cl_2O_8Fe_{0.25}Ni_{0.75}$	fw: 761.45
$a = 10.865(2)$ Å	space group: $R\bar{3}$
$c = 23.65(1)$ Å	$T = 298$ K
$V = 2417(1)$ Å	$\lambda = 0.710\ 73$ Å
$Z = 3$	$\rho_{calc} = 1.567$ g cm^{-3}
$R = 0.054$ (unit weights)[a]	$\mu = 2.24$ mm^{-1}

[a] $R = (\Sigma|F_o - F_c|)/\Sigma F_o$.

Table 2. Selected Bond Lengths (Å) and Angles (deg) for $[Fe_{0.25}Ni_{0.75}(mtz)_6](ClO_4)_2$

Ni1−N1	2.113(3)	N2−N3	1.343(5)
N1−C1	1.316(4)	N2−C2	1.465(6)
N1−N4	1.355(5)	N3−N4	1.287(5)
C1−N2	1.319(5)		
	N1−Ni1−N1′	91.4(1)	

Table 3. Final Significant Coordinates and Equivalent Displacement Parameters ($U_{eq} = (1/3)*\sum_i\sum_j dU_{ij}a_i*a_j*_{ai}a_j$)

atom	*x*	*y*	*z*	U_{eq}
Ni1	0.00000	0.00000	0.00000	0.044(3)
Fe1	0.00000	0.00000	0.00000	0.06(2)
N1	0.1278(3)	0.1804(3)	−0.0503(1)	0.054(1)
C1	0.2648(4)	0.2483(4)	−0.0614(2)	0.056(2)
N2	0.2939(3)	0.3577(3)	−0.0942(1)	0.060(1)
N3	0.1731(4)	0.3599(4)	−0.1036(2)	0.073(2)
N4	0.0736(3)	0.2528(4)	−0.0772(1)	0.066(2)
C2	0.4292(5)	0.4662(5)	−0.1183(2)	0.092(2)
Cl1	0.0000	0.0000	−0.3623(1)	0.0836(8)
O1	0.0144(6)	0.1276(5)	−0.3520(3)	0.183(4)
O2	0.0000	0.0000	−0.4216(5)	0.262(8)

Table 4. Mössbauer Parameters of $[Fe_{0.35}Ni_{0.65}(mtz)_6](ClO_4)_2$ Obtained from a Fit with Lorentzian Lines[a]

	HS(A)			HS(B)			LS		
T (K)	δ (mm/s)	ΔE_Q (mm/s)	$\Gamma/2$ (mm/s)	δ (mm/s)	ΔE_Q (mm/s)	$\Gamma/2$ (mm/s)	δ (mm/s)	$\Gamma/2$ (mm/s)	γ_{HS}
240 ↓	0.98(1)	1.41(2)	0.15(1)						100
220 ↓	0.997(5)	1.424(10)	0.13*				0.407(10)	0.13*	91.3(32)
200 ↓	1.002(4)	1.457(7)	0.121(5)				0.406(6)	0.123(9)	70.7(17)
190 ↓	1.004(5)	1.446(11)	0.123(8)				0.415(5)	0.116(7)	59.0(23)
180 ↓	1.025(5)	1.486(10)	0.122(7)				0.415(2)	0.116(4)	42.9(17)
170 ↓	1.034(7)	1.493(14)	0.119(10)				0.417(2)	0.117(3)	26.8(16)
160 ↓	1.030(24)	1.467(47)	0.125(33)				0.417(3)	0.122(4)	14.3(30)
150 ↓	1.075(32)	1.454(63)	0.12*				0.416(2)	0.120(3)	0.0
100 ↓							0.433(2)	0.132(3)	0.0
50 ↓							0.429(2)	0.125(3)	0.0
10 ↓							0.438(3)	0.144(4)	0.0
40 ↑							0.438(2)	0.145(3)	0.0
50 ↑				1.062(29)	2.45(6)	0.14*	0.436(2)	0.143(3)	8.0(13)
60 ↑				1.065(3)	2.454(5)	0.117(4)	0.429(1)	0.124(2)	35.2(68)
80 ↑				1.062(3)	2.438(7)	0.115(6)	0.427(2)	0.120(2)	37.1(10)
110 ↑				1.053(5)	2.369(9)	0.124(7)	0.418(2)	0.125(3)	36.9(12)
125 ↑				1.040(7)	2.316(13)	0.129(11)	0.427(3)	0.128(4)	37.8(17)
140 ↑				1.039(3)	2.258(7)	0.110(5)	0.412(15)	0.116(3)	37.3(10)
150 ↑	1.087(80)	1.370(14)	0.125*	1.036(3)	2.213(6)	0.117(5)	0.418(1)	0.118(2)	38.6(9)
160 ↑	1.085(73)	1.380(14)	0.125*	1.032(4)	2.170(8)	0.125*	0.405(11)	0.125*	45.1(19)
170 ↑	1.04(1)	1.45(2)	0.125*	1.025(5)	2.13(1)	0.125*	0.405(3)	0.125*	47.6(22)
180 ↑	1.020(6)	1.45(2)	0.125*	0.996(16)	2.10(3)	0.125*	0.403(3)	0.125*	49.6(28)
190 ↑	1.014(4)	1.473(8)	0.125*	1.012(4)	2.07(9)	0.125*	0.399(4)	0.125*	61.1(28)
220 ↑	1.001(5)	1.431(6)	0.13*				0.402(7)	0.13*	89.5(25)

[a] (*) Parameter was not varied; (↓) spectrum was measured in cooling direction; (↑) spectrum was recorded in heating direction.

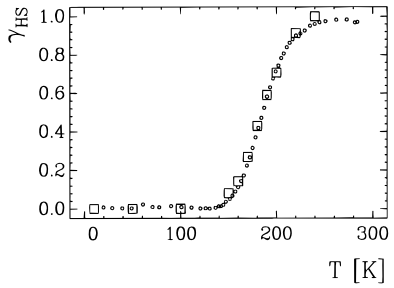

Figure 4. HS fraction γ_{HS} as a function of temperature in $[Fe_{0.35}Ni_{0.65}(mtz)_6](ClO_4)_2$ derived from Mössbauer spectra (□) and magnetic susceptibility measurements (○) in the cooling direction. The measurements prove a complete and gradual spin transition in the temperature range from ca. 220 to ca. 140 K upon cooling.

increasing temperature, whereas the intensities of the LS single line and the HS(B) quadrupole doublet decrease with increasing temperature; a net increase in the total HS fraction is observed with increasing temperature. At 220 K the doublet corresponding to the HS(B) state has completely disappeared, and the spectrum is similar to the one obtained by cooling the complex (cf. Figures 3 and 5). The changes in the Mössbauer spectra in the temperature range from 150 to 220 K can also be followed in the plot of the logarithm of the effective thickness vs temperature (cf. Figure 6), where a discontinuity between 160 and 170 K is observed. Again the Mössbauer investigations were supported by magnetic susceptibility measurements, and the derived spin transition behavior is shown in Figure 7. Obviously, by heating the compound, a two-step transition with a plateau in the temperature range between ca. 75 and ca. 150 K is detected.

3.3. Light-Induced Spin Transition. LIESST experiments were carried out with a polycrystalline sample of $[Fe_{0.35}Ni_{0.65}(mtz)_6](ClO_4)_2$. The sample was first cooled down slowly to 10 K. The Mössbauer spectrum shows a single resonance line arising from the LS state (cf. Figure 8, top). If the crystal is irradiated with green light ($\lambda \sim 350-650$ nm) at 10 K, one observes a partial conversion of the LS state into the HS(A) and HS(B) states, respectively. The HS states can clearly be

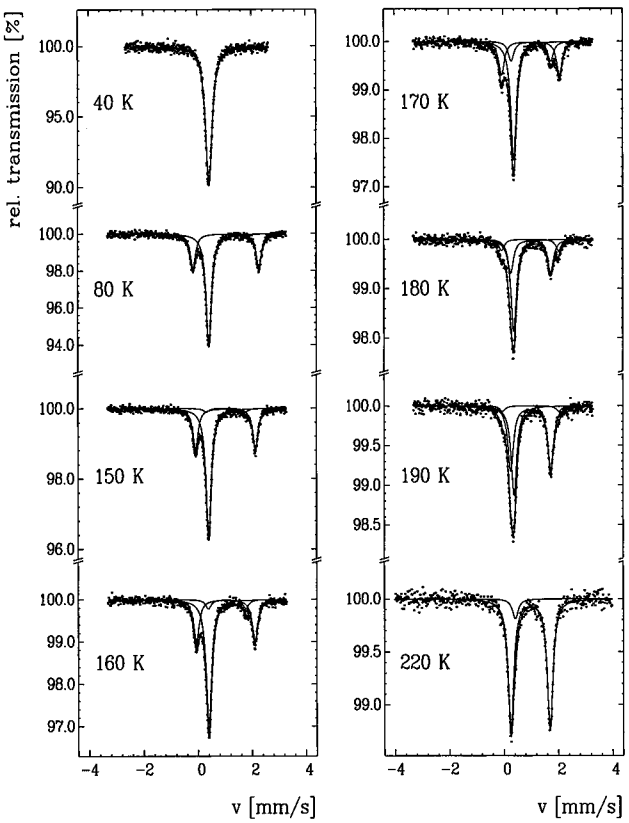

Figure 5. Mössbauer spectra of $[Fe_{0.35}Ni_{0.65}(mtz)_6](ClO_4)_2$ recorded in heating direction. At 40 K only the resonance line of the LS state is detected. At temperatures between ca. 50 and ca. 75 K a HS(B) state is populated leading to a total HS fraction of ~37% at 80 K. At 150 K another HS state (HS(A)) is detected. The intensity of the resonance lines of this HS state increases with increasing temperatures, whereas the intensity of the resonance lines of the LS and HS(B) decreases. At 220 K the HS(B) has completely disappeared and the spectrum is similar to the one recorded by initial cooling of the compound.

distinguished in the Mössbauer spectra due to the different quadrupole splittings of the doublets (cf. Table 5 and Figure 8,

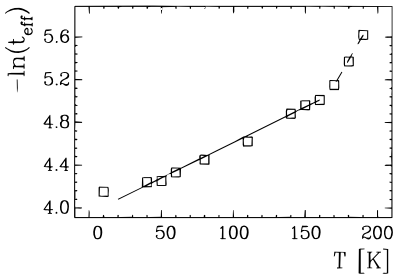

Figure 6. ln t_{eff} vs T plot measured in the heating direction. The plot deviates from the expected linearity; the discontinuity between 160 and 170 K indicates the onset of a structural phase transition.

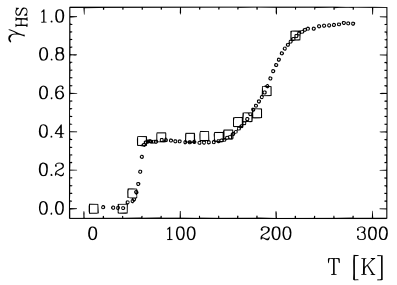

Figure 7. HS fraction γ_{HS} as a function of temperature in $[Fe_{0.35}Ni_{0.65}(mtz)_6](ClO_4)_2$ derived from Mössbauer spectra (□) and magnetic susceptibility measurements (○) in the heating direction. The spin transition curve shows a plateau in the temperature range from ca. 75 to ca. 150 K.

bottom). The relaxation behavior of the HS states is quite different. It was found that the HS(A) shows a relaxation to the LS state even at 10 K (complete relaxation within 7 h at 15 K). Therefore, a quantitative LS → HS conversion could not be observed with Mössbauer spectroscopy. Mössbauer spectra recorded after LIESST and subsequent heating of the complex are depicted in Figure 9. From the spectrum at 30 K it can be clearly seen that the HS(A) state has disappeared. The HS(B) state shows no noticeable relaxation at temperatures below 60 K (cf. Figure 9, spectra at 30 and 50 K). Only at 60 K a very slow HS → LS relaxation of this HS state (within days) leading to the HS fraction corresponding to the thermal equilibrium value was observed. The Mössbauer spectrum recorded at 75 K after LIESST at 10 K and subsequent heating to 75 K shows no difference from the spectrum recorded after slowly cooling to 20 K and subsequent heating to 75 K.

No long-lived metastable HS states could be generated at temperatures above 60 K. Reverse LIESST experiments on HS(B) using red light were carried out at 20 K after complete relaxation of the HS(A) state. After irradiation of the sample with red light a reduction of only 10% of the HS intensity was observed, proving that a partial back conversion from the HS(B) to the LS state has occurred.

4. Discussion

The investigation of the spin transition behavior in the present compound revealed that apparently an additional phase transition occurs when the compound is cooled to temperatures below 60 K. Therefore, the spin transition behavior in the high- and low-temperature structure should be discussed separately.

In the high-temperature structure ($R\bar{3}$) all iron atoms are equivalent, and therefore only one HS doublet is observed in the Mössbauer spectra. In this structure a complete and gradual spin transition is detected due to the reduced cooperative interaction between the spin-changing molecules caused by the nickel matrix; this effect is well-known from other metal dilution studies.[8,9,19,20]

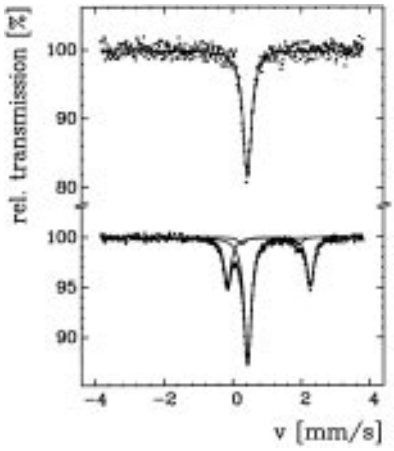

Figure 8. ^{57}Fe Mössbauer spectra of $[Fe_{0.35}Ni_{0.65}(mtz)_6](ClO_4)_2$ recorded at 10 K before (top) and after (bottom) irradiation of the sample with green light. Two different metastable HS states are populated by irradiating the compound.

The spin transition behavior in the low-temperature structure is completely different. From the Mössbauer measurements we can state that there are at least two inequivalent positions for the iron atoms in this structure.

The quadrupole splittings observed at 10 K for these atoms, after irradiation with green light (LIESST), are ca. 3 and 1.5 mm/s, which is the low-temperature value for iron(II) complexes with ground states with 1- and 2-fold orbital degeneracy, respectively.[21] The most interesting feature of the spin transition behavior in the low-temperature structure is the plateau in the spin transition curve between ca. 75 and ca. 150 K. Some other complexes are known, where a plateau in the spin transition curve was observed.[22,23] In the case of the spin crossover compound $[Fe(2\text{-pic})_3]Cl_2 \cdot EtOH$, the iron(II) ions occupy equivalent lattice positions;[24] the origin of the two-step spin transition in this case is presumably due to short-range interactions, leading to correlations of HS and LS states deviating from a random distribution.[25] In the present compound, however, one must assume that the iron atoms are located in different environments, which apparently cause the different spin transition temperature. A similar situation is known for the $[Fe(mtz)_6]X_2$ ($X = BF_4^-$, ClO_4^-) complexes, where the iron atoms occupy two different lattice sites A and B, which are only slightly different.[26] The complexes at lattice site A show a HS → LS transition at temperatures below 100 K, whereas the complexes at lattice site B stay in the HS state even at 4.2 K.[27,28] The plateau in the spin transition curve in the present example most probably arises from two successive spin transitions with different spin transition temperatures $T_{1/2}(\gamma_{HS} = 0.5)$, the spin transition in lattice site A at higher temperatures and the spin transition in lattice site B at lower temperatures.

(19) Martin, J. P.; Zarembowitch, J.; Dworkin, A.; Haasnoot, J. G.; Codjovi, E. *Inorg. Chem.* **1994**, *33*, 2617.
(20) Martin, J. P.; Zarembowitch, J.; Bousseksou, A.; Dworkin, A.; Haasnoot, J. G.; Varret, F. *Inorg. Chem.* **1994**, *33*, 6325.
(21) Ganiel, U. *Chem. Phys. Lett.* **1969**, *4*, 87.
(22) Köppen, H.; Müller, E. W.; Köhler, C. P.; Spiering, H.; Meissner, E.; Gütlich, P. *Chem. Phys. Lett.* **1982**, *91*, 348.
(23) Petrouleas, V.; Tuchagues, J. P. *Chem. Phys. Lett.* **1987**, *137*, 21.
(24) Mikami, M.; Konno, M.; Saito, Y. *Chem. Phys. Lett.* **1979**, *63*, 566.
(25) Jakobi, R.; Spiering, H.; Gütlich, P. *J. Phys. Chem. Solids* **1992**, *53*, 267.
(26) Wiehl, L. *Acta Crystallogr. Sect. B* **1993**, *49*, 289.
(27) Poganiuch, P.; Decurtins, S.; Gütlich, P. *J. Am. Chem. Soc.* **1990**, *112*, 3270.
(28) Buchen, Th.; Poganiuch, P.; Gütlich, P. *J. Chem. Soc., Dalton Trans.* **1994**, 2285.

Table 5. Mössbauer Parameters of $[Fe_{0.35}Ni_{0.65}(mtz)_6](ClO_4)_2$ before and after Irradiation with Green Light[a]

	HS(A)			HS(B)			LS		
T	δ (mm/s)	ΔE_Q (mm/s)	$\Gamma/2$ (mm/s)	δ (mm/s)	ΔE_Q (mm/s)	$\Gamma/2$ (mm/s)	δ (mm/s)	$\Gamma/2$ (mm/s)	γ_{HS}
10 K before LIESST							0.436(4)	0.148(6)	0.0
10 K after LIESST	1.11(2)	1.65(4)	0.125*	1.066(3)	2.419(6)	0.125*	0.444(2)	0.125*	46.9(14)
30 K after LIESST				1.070(4)	2.443(7)	0.119(6)	0.425(2)	0.128(3)	39.8(11)
50 K after LIESST				1.078(6)	2.458(12)	0.125(10)	0.434(2)	0.129(3)	38.7(15)
75 K after LIESST				1.059(5)	2.435(9)	0.129(7)	0.435(2)	0.133(3)	38.3(5)

[a] (*) Parameter was not varied.

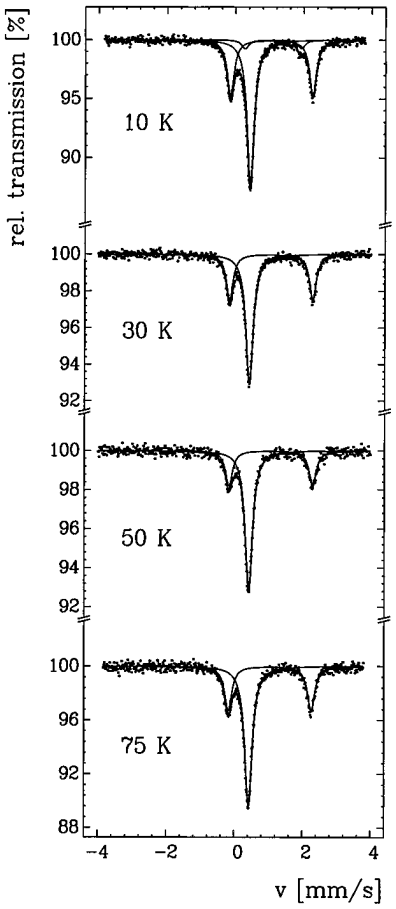

Figure 9. Mössbauer spectra of $[Fe_{0.35}Ni_{0.65}(mtz)_6](ClO_4)_2$ recorded at 10 K after irradiation with green light and subsequent heating of the complex. At 10 K the two metastable HS states A and B are detected in the Mössbauer spectrum. The HS(A) state shows HS → LS relaxation even at 10 K; in the spectrum recorded at 30 K this HS state has completely disappeared and only the HS(B) and the LS state are observed. The HS(B) state shows no relaxation at temperatures below 60 K. The 75 K spectrum resembles the one measured at this temperature in the heating direction.

The change from the low- to the high-temperature structure is observed between ca. 170 and 200 K in the heating mode. We concluded this from the changes in the Mössbauer spectra (disappearance of HS(B)) and from the unexpected behavior of the $\ln(t_{eff})$ vs T plot, which shows a discontinuity between 160 and 170 K, indicating the onset of a structural phase transition. It would be desirable to investigate the structural changes directly by diffraction methods because a comparison of the high- and low-temperature structure should give an insight into the mechanism which is responsible for the dramatic changes in the Mössbauer spectra and in the spin transition behavior. The high-temperature structure could be determined by X-ray crystallography of the isomorphous complex $[Fe_{0.25}Ni_{0.75}(mtz)_6](ClO_4)_2$. But up to now we were not in the position to perform an X-ray structural analysis on single crystals in the very low temperature region ($T \leq 60$ K). However, we could measure temperature dependent X-ray powder diffraction patterns, which should also enable us to obtain some information about the structural changes. As it is well-known that the spin transition behavior is strongly influenced by grinding effects,[29−31] the spin transition behavior of the powdered sample was checked and turned out to be similar to the behavior which was observed for the polycrystalline sample. Thus, there was no additional change on the spin transition behavior introduced by grinding the sample. The high-temperature structure of $[Fe_{0.25}Ni_{0.75}(mtz)_6](ClO_4)_2$ was then used to assign the reflexes in the powder diffraction pattern at high temperatures. Characteristic changes in the X-ray diffraction pattern were observed in the region of the (101) reflex at ~60 K and between ca. 170 and 200 K for cooling and heating, respectively (cf. Figure 10 for heating direction), which agrees with the changes seen in the Mössbauer and magnetic measurements in the same temperature regions. Therefore, we believe that the observed changes in the X-ray powder measurements reflect the structural changes of the compound at these temperatures. Whatever the process behind this phenomenon is, the nickel concentration apparently plays a significant role. The intensity of the HS(B) state increases with increasing nickel content of the mixed crystals, and the phase transition is no longer observed for mixed crystals with a nickel content of ≤55%.

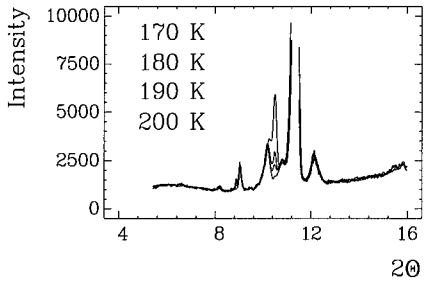

Figure 10. X-ray powder spectra of $[Fe_{0.35}Ni_{0.65}(mtz)_6](ClO_4)_2$ recorded at 170, 180, 190, and 200 K in the heating direction with the (101), (003), and (102) reflexes at $2\theta = 10.267°$, 11.387°, and 12.154° at 170 K. Characteristic changes in the region of the (101) reflex are observed in this temperature region which agree with the changes seen in the Mössbauer and magnetic measurements in the same temperature regions.

The LIESST experiments in the low-temperature structure yielded two different HS states, for which a different relaxation behavior was observed. The HS → LS relaxation kinetics after laser excitation was carefully studied by Hauser in a series of iron(II) complexes with an $Fe-N_6$ core.[4,32−34] He observed a thermally activated relaxation behavior at elevated temperatures and a nearly temperature independent tunnelling mechanism for the HS → LS relaxation at low temperatures. The low-temperature tunnelling rate depends, on one hand, on the so-

(29) Haddad, M. S.; Federer, W. D.; Lynch, M. W.; Hendrickson, D. N. *Inorg. Chem.* **1981**, *20*, 131.
(30) Müller, E. W.; Spiering, H.; Gütlich, P. *Chem. Phys. Lett.* **1982**, *93*, 567.
(31) Müller, E. W.; Spiering, H.; Gütlich, P. *Inorg. Chem.* **1984**, *23*, 119.

called Huang−Rhys factor, which is a measure of the horizontal displacement of the potentials of the HS and LS state and, on the other hand, the energy gap between the HS and LS states (the difference between the lowest vibronic levels of the HS and LS state). In iron(II) complexes with $Fe-N_6$ cores the crucial parameter for the tunnelling rate is the energy gap. Although the spin transition temperature $T_{1/2}$ is only a crude measure for this gap, Hauser observed an increase in the low-temperature tunnelling rate with increasing $T_{1/2}$ (inverse energy gap law). The relaxation behavior found for $[Fe_{0.35}Ni_{0.65}(mtz)_6](ClO_4)_2$ agrees qualitatively with Hauser's relaxation model. For the iron complexes on site A $T_{1/2}$ is 185 K, whereas $T_{1/2}$ for the complexes on site B is around ∼60 K, so that a faster relaxation for the light-induced metastable HS(A) state is predicted and in fact observed.

At temperatures below 50 K the HS → LS relaxation of the HS(B) state is very slow and no relaxation could be observed within days using Mössbauer spectroscopy; the HS state generated by light is kinetically stable. In this temperature range reverse LIESST experiments on HS(B) are possible. The fact that we achieved only a partial HS(B) → LS(B) back conversion is most likely due to the broad band irradiation using a xenon-arc lamp and filters leading to a simultaneous excitation of the HS and the LS state. This effect has been discussed in detail in ref 27. At 60 K a very slow relaxation is observed toward the HS fraction reached in the course of the thermal spin transition. This proves that the generated HS(B) state is a metastable state at temperatures below 60 K. But at 60 K the HS(B) state becomes already thermodynamically stable (see thermal spin transition curve in Figure 7) so that no complete decay of the HS(B) can be observed. This is obviously due to overlapping regions of kinetic and thermodynamical stability of the HS(B) state.

Acknowledgment. We wish to acknowledge the financial support from the Deutsche Forschungsgemeinschaft, the Bundesministerium für Forschung and Technologie, the Fonds der Chemischen Industrie, and the Materialwissenschaftliches Forschungszentrum of the University of Mainz. We thank G. Schmitt for his assistance in the recording and evaluation of the X-ray powder diffraction pattern.

Supporting Information Available: Tables of the detailed crystallographic data, final coordinates and equivalent displacement parameters for non-hydrogen atoms, anisotropic displacement parameters for non-hydrogen atoms, final coordinates and isotropic displacement parameters for the hydrogen atoms, and all distances, angles, and torsion angles for $[Fe_{0.25}Ni_{0.75}(mtz)_6](ClO_4)_2$ (7 pages). Ordering information is given on any current masthead page.

IC9504405

(32) Hauser, A.; Vef, A.; Adler, P. *J. Chem. Phys.* **1991**, *95*, 8710.
(33) Hauser, A. *J. Chem. Phys.* **1991**, *94*, 2741.
(34) Hauser, A. *Chem. Phys. Lett.* **1992**, *192*, 65.